Supporting Information

Rational Design of Metallophosphors with Tunable Aggregation-Induced Phosphorescent Emission and Their Promising Applications in Time-Resolved Luminescence Assay and Targeted Luminescence Imaging of Cancer Cells

By Shujuan Liu,[‡a] Huibin Sun,[‡a] Yun Ma,[a] Shanghui Ye,[a] Xiangmei Liu,[a] Xinhui Zhou,[a] Xin Mou,[a] Lianhui Wang,[a] Qiang Zhao*[ab] and Wei Huang*[a]

[a]Key Laboratory for Organic Electronics & Information Displays (KLOEID) and Institute of Advanced Materials (IAM), Nanjing University of Posts and Telecommunications, No. 9 WenYuan Road, Nanjing, 210046 (P. R. China)
[b]State Key Laboratory of Coordination Chemistry, Nanjing University, Nanjing, 210093 (P. R. China).

* Correspondence: iamqzhao@njupt.edu.cn; wei-huang@njupt.edu.cn. Fax: +86 25 8586 6008; Tel: +86 25 8586 6008.

Table of Contents

Experimental Section

Materials: All starting materials were purchased from commercial sources and used as received. 2-Phenylpyridine was purchased from Aldrich Chemical Co. All other ligands and materials were purchased from either Aldrich Chemical Co. or Acros. The solvents used for synthesis were of analytical grade unless stated otherwise.

Characterization: ^{1}H NMR spectra were recorded on a Bruker Ultra Shield Plus 400MHz NMR instruments. Mass spectra were obtained on a Bruker autoflex MALDI-TOF/TOF or LCQ Fleet ESI mass spectrometer. Photoluminescent spectra were measured using a RF-5301PC spectrofluorophotometer. The UV-visible absorption spectra were recorded on a Shimadzu UV-3600 UV-VIS-NIR spectrophotometer. The quantum efficiency of the complexes in crystal state was determined through an absolute method by employing an integrating sphere. Lifetime studies were performed with an Edinburgh FL 920 photocounting system with a hydrogen-filled lamp as the excitation source. Time-resolved emission spectra (TRES) were acquired through a time-correlated single photon counting (TCSPC) technique by using an Edinburgh FL 920 instrument.

Time-Gated Photoluminescence: Time-gated acquisition of photoluminescence spectra was performed by employing the TRES technique. Delayed photoluminescence spectra acquired after 160 ns did not contain fluorescence originating from fluorescein. Thus, a photoluminescence spectrum at 166 ns delay was chosen and compared with the total photoluminescence spectrum.

Synthesis of Pt(II) Complexes: Ancillary ligand was synthesized according to a procedure modified from that reported in the literature.[1] A EtOH solution (8.0 mL) dissolved by salicylaldehyde (2.3 mL, 22.0 mmol) was added to a stirred EtOH solution (40 mL) of aniline (2.0 mL, 22.0 mmol). After adding catalytic amount of AcOH, the reaction mixture was stirred at room temperature for 2 hr. Concentration and subsequent silica gel column

purification gave yellow solid (3.90 g, 19.8 mmol, 92% yield). Same procedures of L1, L3, L4 and L5 (see Scheme 1) were applied for this synthesis to give yellow powder or liquid. The yields of these complexes were quantitative (> 90%).

All Pt(II) complexes were synthesized according to the same procedure.[2,3] Pt(II) μ-dichloro-bridged dimers were synthesized from the starting materials of K_2PtCl_4 and C^N ligand according to the previous report.[2] A solution of Pt(II) μ-dichloro-bridged dimers, 3 equiv of the ancillary ligand and 10 equiv of Na_2CO_3 in 2-ethoxyethanol was heated to reflux for 16 h. Then the reaction mixture was concentrated under reduced pressure. Excess of water was added gradually to give orange or red precipitate of crude product that was subsequently filtered and washed with water. The obtained crude product was purified by silica gel column chromatography using dichloromethane as the eluent to give pure products with moderate yield (28% to 54%).

Characterization of Ancillary Ligands:

2-(Phenyliminomethyl)-phenol (L1). ^{1}H NMR (500 MHz, $CDCl_3$) δ: 6.87 (t, J = 7.6 Hz, 1H,), 6.99 (d, J = 8.2 Hz, 1H), 7.21 (m, 3H), 7.30 (d, J = 7.5 Hz, 2H), 7.35 (t, J = 7.5 Hz, 2H), 8.50 (s, 1H), 13.3 (s, 1H). ^{13}C NMR (125 MHz, $CDCl_3$) δ: 117.29, 119.11, 119.28, 121.25, 126.97, 129.45, 132.40, 133.18, 148.37, 161.23, 162.69.

2-(Naphthyliminomethyl)-phenol) (L2). ^{1}H NMR (400 MHz, $CDCl_3$) δ = 13.41 (s, 1H; Ar-OH), 8.71 (s, 1H; N=CH), 8.27-8.29 (m, 1H; Ar-H), 7.83-7.91 (m, 1H; Ar-H), 7.79 (d, *J* = 8.29 Hz, 1H; Ar-H), 7.42-7.59 (m, 5H; Ar-H), 7.18 (d, *J* = 7.27 Hz,1H; Ar-H), 7.11 (d, *J* = 8.18 Hz,1H; Ar-H), 7.0(t, *J* = 7.46 Hz,1H; Ar-H). ^{13}C NMR (100 MHz, $CDCl_3$): δ = 114.04, 117.34, 119.24, 119.54, 123.27, 125.96, 126.53, 126.72, 126.96, 127.94, 128.25, 132.44, 133.44, 134.01, 146.24, 161.26, 163.65.

2-(Propyliminomethyl)-phenol (L3). ^{1}H NMR (400 MHz, $CDCl_3$) δ = 13.63 (s, 1H; Ar-OH) 8.33 (s, 1H; N=CH), 7.23-7.32 (m, 2H; Ar-H), 6.95 (d, *J* = 8.24 Hz, 1H; Ar-H), 6.87 (t, *J* = 7.37 Hz, 1H; Ar-H), 3.56 (t, *J* = 6.80 Hz, 2H; N-CH_2), 1.68-1.77 (m, 2H; CH_2), 0.98(t, *J* =

7.38 Hz, 3H; CH_3). ^{13}C NMR (100 MHz, $CDCl_3$): δ = 11.72, 24.10, 61.19, 117.02, 118.39, 118.87, 131.20, 132.04, 161.51, 164.86.

1-((Phenylimino)methyl)naphthalen-2-ol (L4). ^{1}H NMR (400 MHz, $CDCl_3$) δ = 15.51 (s, 1H; Ar-OH), 9.30 (s, 1H; N=CH), 8.08 (d, *J* = 8.44 Hz, 1H; Ar-H), 7.79 (d, *J* = 9.20 Hz, 1H; Ar-H), 7.70 (d, *J* = 7.93 Hz, 1H; Ar-H), 7.44-7.53 (m, 3H; Ar-H), 7.27-7.38 (m, 4H; Ar-H), 7.08(d, *J* = 9.20 Hz,1H; Ar-H). ^{13}C NMR (100 MHz, $CDCl_3$): δ = 108.76, 118.82, 120.23, 122.50, 123.55, 126.53, 127.27, 128.12, 129.41, 129.71, 133.31, 136.87, 145.01, 154.40, 170.93.

Characterization of Pt(II) Complexes 1-9:

Pt(ppy)(L1) (1). Yield: 54%. ^{1}H NMR (400 MHz, $CDCl_3$): δ = 9.55(d, *J* = 5.02 Hz, 1H), 8.25(s, 1H), 7.8(t, *J* = 6.30 Hz, 1H), 7.6(m, 3H), 7.47(t, *J* = 6.80 Hz, 1H), 7.39(m, 3H), 7.31(m, 2H), 7.23(m, 1H), 7.08(d, *J* = 8.55 Hz, 1H), 6.86(t, *J* = 6.88 Hz, 1H), 6.56(m, 2H), 5.68(d, *J* = 7.08 Hz,1H). ^{13}C NMR (100 MHz, $CDCl_3$): δ = 115.65, 118.23, 120.83, 121.99, 122.72, 122.79, 123.03, 125.74, 127.35, 128.60, 128.97, 128.99, 131.07, 134.53, 135.55, 138.49, 138.78, 145.60, 146.56, 154.88, 163.47, 165.91, 167.91. MS (MALDI-TOF/TOF): m/z 546.169 $[[M+H]^+]$.

Pt(ppy)(L2) (2). Yield: 49%. ^{1}H NMR (400 MHz, $CDCl_3$): δ = 9.66(d, *J* = 5.78 Hz, 1H), 8.48(d, *J* = 8.20 Hz, 1H), 8.29(s, 1H), 7.85-7.98(m, 3H), 7.75-7.82(m, 1H), 7.45-7.6(m, 7H), 7.29(m, 2H), 7.16(d, *J* = 8.55 Hz, 1H), 6.73(t, *J* = 7.41 Hz, 1H), 6.6(t, *J* = 7.35 Hz, 1H), 6.26(t, *J* = 7.18 Hz, 1H). ^{13}C NMR (100 MHz, DMSO): δ = 115.04, 118.70, 121.35, 121.37, 121.48, 121.90, 122.46, 122.77, 123.21, 125.40, 126.44, 126.49, 127.39, 127.55, 127.86, 128.55, 132.31, 133.57, 135.20, 135.45, 136.81, 139.77, 145.40, 145.74, 150.91, 164.53, 164.70, 166.63. MS (MALDI-TOF/TOF): m/z 596.250 $[[M+H]^+]$.

Pt(ppy)(L3) (3). Yield: 28%. ^{1}H NMR (400 MHz, $CDCl_3$): δ = 9.39(d, *J* = 5.35 Hz, 1H), 7.90(s, 1H), 7.81(t, *J* = 7.34 Hz, 1H), 7.63(d, *J* = 8.04 Hz, 1H), 7.45(t, *J* = 8.28 Hz, 2H), 7.34(t, *J* = 8.58 Hz, 1H), 7.19-7.23(m, 2H), 7.05-7.13(m, 2H), 7.00(d, *J* = 8.47 Hz, 1H),

6.54(t, *J* = 7.65 Hz, 1H), 4.29(t, *J* = 7.26 Hz, 2H), 1.88-1.96(m, 2H), 0.93(t, *J* = 7.38 Hz, 3H). ^{13}C NMR (100 MHz, $CDCl_3$): δ = 11.16, 27.49, 67.08, 115.09, 118.20, 120.95, 122.03, 122.81, 123.00, 123.57, 129.45, 133.57, 134.68, 134.87, 138.53, 139.53, 146.14, 146.53, 162.38, 166.62, 167.48. MS (ESI): m/z 512.33 [$[M+H]^+$].

Pt(dfppy)(L1) (4). Yield: 52%. ^{1}H NMR (400 MHz, $CDCl_3$): δ = 9.60(d, *J* = 6.18 Hz, 1H), 8.23(s, 1H), 8.01(d, *J* = 8.34 Hz, 1H), 7.84(t, *J* = 7.72 Hz, 1H), 7.58(d, *J* = 7.46 Hz, 2H), 7.48(t, *J* = 6.88 Hz, 1H), 7.42(t, *J* = 7.46 Hz, 2H), 7.32-7.38(m, 2H), 7.27-7.29(m, 1H), 7.10(d, *J* = 8.57 Hz, 1H), 6.62(t, *J* = 7.37 Hz, 1H), 6.35(t, *J* = 9.46 Hz, 1H), 5.17 (d, *J* = 8.69 Hz, 1H). ^{13}C NMR (100 MHz, $CDCl_3$): δ = 98.64, 115.86, 116.76, 120.55, 121.67, 121.86, 122.06, 122.43, 125.59, 127.60, 129.04, 134.39, 135.71, 139.18, 142.91, 146.45, 149.61, 154.02, 163.54, 164.52, 164.58, 165.59. MS (MALDI-TOF/TOF): m/z 581.154 [M^+].

Pt(dfppy)(L2) (5). Yield: 48%. ^{1}H NMR (400 MHz, $CDCl_3$) δ = 9.71(d, *J* = 4.88 Hz, 1H), 8.50(d, *J* = 8.31 Hz, 1H), 8.30(s, 1H), 7.92-7.98(m, 3H), 7.82(t, *J* = 7.25 Hz, 1H), 7.45-7.60(m, 6H), 7.28-7.31(m, 2H), 7.17(d, *J* = 8.29 Hz, 1H), 6.63(t, *J* = 6.88 Hz, 1H), 6.18-6.24 (m, 1H). ^{13}C NMR (100 MHz, $CDCl_3$): δ = 98.66, 115.84, 120.42, 121.27, 121.68, 121.73, 121.94, 122.54, 123.15, 125.23, 126.86, 126.88, 128.01, 128.15, 128.97, 129.27, 134.18, 134.54, 135.87, 139.14, 141.32, 146.46, 150.76, 160.37, 162.76, 164.49, 164.58, 165.37. MS (MALDI-TOF/TOF): m/z 632.081 [$[M+H]^+$].

Pt(dfppy)(L3) (6). Yield: 37%. ^{1}H NMR (400 MHz, $CDCl_3$): δ = 9.38(d, *J* = 5.80 Hz, 1H), 7.98(d, *J* = 8.30 Hz, 1H), 7.81-7.85(m, 2H), 7.36(t, *J* = 8.60 Hz, 1H), 7.20-7.24(m, 2H), 7.01(d, *J* = 8.45 Hz, 1H), 6.88(d, *J* = 7.37 Hz, 1H),6.51-6.59(m, 2H), 4.20(t, *J* = 7.25 Hz, 2H), 1.88-1.93(m, 2H), 0.93(t, *J* = 7.38 Hz, 3H). ^{13}C NMR (100 MHz, $CDCl_3$): δ = 11.04, 27.51, 66.52, 98.85, 115.40, 116.87, 120.76, 121.79, 122.06, 122.66, 129.47, 133.46, 135.05, 139.02, 144.33, 146.37, 158.77, 161.40, 162.61, 164.15, 166.33. MS (MALDI-TOF/TOF): m/z 548.165 [$[M+H]^+$].

Pt(Fiq)(L1) (7). ^{1}H NMR (400 MHz, $CDCl_3$) δ = 9.50(d, J = 6.54 Hz, 1H), 8.76(d, J = 8.57 Hz, 1H), 8.36(s, 1H), 7.90(d, J = 7.91 Hz, 1H), 7.77(t, J = 7.84 Hz, 4H), 7.67(t, J = 7.18 Hz, 1H), 7.48-7.56(m, 4H), 7.40(t, J = 7.38 Hz, 1H), 7.35(d, J = 6.23 Hz, 1H), 7.23-7.25(m, 3H), 7.15(d, J = 8.51 Hz, 1H), 7.08-7.10(m, 1H), 6.61(t, J = 7.82 Hz, 1H), 6.27(s, 1H), 1.81-1.93(m, 4H), 1.02-1.25(m, 24H), 0.78(t, J = 7.05 Hz, 6H). ^{13}C NMR (100 MHz, $CDCl_3$): δ = 14.04, 22.56, 23.99, 29.22, 29.26, 30.08, 31.78, 40.13, 54.48, 115.49, 117.85, 120.34, 121.91, 122.65, 122.82, 123.61, 125.27, 125.99, 126.06, 126.44, 127.04, 127.34, 127.57, 127,72, 128.97, 131.21, 134.35, 135.34, 137.88, 137.97, 138.95, 140.89, 142.20, 144.74, 145.59, 151.89, 154.95, 157.88, 163.26, 165.94, 169.52. MS (MALDI-TOF/TOF): m/z 907.819 [M^+].

Pt(ppy)(L4) (8). Yield: 35%. ^{1}H NMR (400 MHz, $CDCl_3$): δ = 9.48(d, *J* = 5.22 Hz, 1H), 8.91(s, 1H), 7.79-7.84(m, 3H), 7.73(d, *J* = 7.63 Hz, 2H), 7.68(d, *J* = 7.59 Hz, 7H), 7.62(d, *J* = 8.02 Hz, 2H), 7.31-7.50(m, 6H), 7.22-7.25(m, 2H), 6.89(t, *J* = 7.23 Hz, 1H), 6.62(t, *J* = 7.01 Hz, 1H), 5.87(d, *J* = 7.84 Hz, 1H). ^{13}C NMR (100 MHz, $CDCl_3$): δ = 112.77, 118.22, 119.85, 120.83, 122.57, 122.74, 122.93, 125.57, 126.07, 126.98, 127.25, 127.62, 128.71, 128.90, 128.95, 134.52, 134.68, 135.85, 138.51, 138.60, 145.39, 146.30, 155.23, 157.70, 166.46, 167.72. MS (MALDI-TOF/TOF): m/z 595.157 [M^+].

Pt(dfppy)(L4) (9). Yield: 33%. ^{1}H NMR (400 MHz, $CDCl_3$) δ = 9.50(d, *J* = 5.80 Hz, 1H), 8.93(s, 1H), 8.11-8.18(m, 3H), 7.86(d, *J* = 7.68 Hz, 2H), 7.80(d, *J* = 7.83 Hz, 1H), 7.46-7.60(m, 5H), 7.34(t, *J* = 7.30 Hz, 1H), 7.30(m, 2H), 6.73(t, *J* = 9.59 Hz, 1H), 5.32(dd, *J* = 2.46, 2.24 Hz, 1H). ^{13}C NMR (100 MHz, $CDCl_3$): δ = 98.68, 112.60, 116.90, 119.99, 120.66, 121.95, 122.15, 122.80, 125.23, 126.00, 127.31, 127.77, 129.00, 129.03, 129.70, 134.34, 135.15, 139.09, 143.00, 146.25, 154,49, 157.83, 160.92, 164.45, 166.22, 171.15. MS (MALDI-TOF/TOF): m/z 631.408 [M^+].

Synthesis of 1-PNPs-FA: Sodium dodecylsulfate (SDS, 150 mg) and deionized water (55 mL) were mixed in a 100 mL beaker, and then an amount of styrene (2g) containing **1** (8.0 mg) and azodiisobutyronitrile (AIBN, 45 mg) was added. The emulsion was obtained by

ultrasonic treatment for 30 min. Then, the emulsion was added into a flask and degassed by nitrogen for 30 min. Subsequently, the temperature was heated to 65 °C and 1 mL deionized water containing 20 mg acrylamide was injected into the reaction solution after 1 h. The reaction was allowed to proceed for 24 h. The resulting **1**-PNPs were precipitated by NaCl aqueous solution (1 mol L^{-1}), and the particles were purified by repeated centrifugation–redispersion cycles using ethanol and deionized water three times. To modify the **1**-PNPs with FA, FA (110.35 mg, 0.25 mmol) was dissolved in dimethyl sulfoxide (DMSO; 80 mL) and then activated with 3-(3-dimethylaminopropyl)-1-ethylcarbodiimide (EDC) and *N*-hydroxysuccinimide (NHS) (with a molar ratio of FA/EDC/NHS equivalent to 1:1:2.5) under N_2 at room temperature for 1h. **1**-PNPs (100mg, 0.05mmol) dissolved in DMSO (50 mL) were added to the activated FA solution, and mixture was stirred gently for 3 h at room temperature in dark. The obtained **1**-PNPs-FA were purified by centrifugation at 8000 rpm for 8 min and washed 3-4 times with PBS (pH 7.4).

X-ray Crystallography Analysis. The crystal structures of complex **1-3**, **5** and **8** were determined on a Siemens (Bruker) SMART CCD diffractometer using monochromated Mo-Kα radiation (λ = 0.71073 Å) at room temperature. The structure was solved by direct methods and refined by full-matrix least-squares on F^2 using the program SHELXL-97.[4] All non-hydrogen atoms were refined anisotropically. Hydrogen atoms were placed in calculated position and refined as riding atoms with a uniform value of U_{iso}. For the full-matrix least-squares refinements [$I > 2\sigma(I)$], the unweighted and weighted agreement factors of $R_1 = \Sigma||F_o| - |F_c||/\Sigma|F_o|$ and $wR_2 = [\Sigma w(F_o^2 - F_c^2)^2/\Sigma w(F_o^2)]^{1/2}$ were used. CCDC reference numbers for **1-3**, **5** and **8** is 808311, 808312, 808313, 808310, and 808314, respectively.

Theoretical Calculations: Density functional theory (DFT) calculations were employed to investigate the nature of the low-lying excited electronic states in these complexes. The ground state (S0) was fully optimized at the B3LYP levels. On the basis of ground-state optimization, the time-dependent density functional theory (TDDFT) approach was applied to

study their absorptions and emissions in solution. The LANL2DZ and 6-31G(d) basis sets were employed for the Pt(II) atom and the other atoms, respectively. The molecular structure and crystal structure of complexes **1**, **2**, **3**, **5** and **8** were optimized using DFT calculations with the double numerical basis set with polarization functions (DNP) and the generalized gradient corrected Perdew-Burke-Ernzerhof (GGA-PBE) functional implemented in the DMol3 package.[5-7] The core electrons of all atoms were represented by semi-core pseudopotentials (DSPP).[8] The Brillouin zone was sampled only by Gamma-point. Geometry optimization was performed using the Broyden-Fletcher-Goldfarb-Shanno algorithm with a convergence criterion of 5×10^{-3} hartree on the displacement and 4×10^{-3} hartree on the gradient and 1×10^{-4} hartree on the total energy.

Cell Culture: The human cervical carcinoma cell line (HeLa cells) was supplied by the Institute of Biochemistry and Cell Biology, SIBS, CAS (China). The HeLa cells were grown in RPMI 1640 (Roswell Park Memorial Institute's Medium) supplemented with 10% FBS (Fetal Bovine Serum) at 37 °C and 5% CO_2. Cells (5×10^8/L) were plated on 18mm glass coverslips and allowed to adhere for 24 h.

Cytotoxicity Assay: The cytotoxicity of the **1**-PNPs-FA toward the HeLa cells has been determined by the methyl thiazolyl tetrazolium (MTT) assay. Before incubated at 37 °C under 5% CO_2 atmosphere for 24 h, HeLa cells in log phase were seeded into a 96-well cell-culture plate at 1×10^4/well. The **1**-PNPs-FA at concentrations of 1, 0.5, 0.25, 0.125 mg mL^{-1} was added to the wells of the treatment group. The cells incubated at 37 °C under 5% CO_2 atmosphere for 24 h. 20 μL MTT solution (5 mg/mL) was added to each well of the 96-well assay plate, and the solution was incubated for another 3 h under the same condition. A Tecan Infinite M200 monochromator based multifunction microplate reader was used for measuring the OD570 (Absorbance value) of each well referenced at 690 nm. The following formula was used to calculate the viability of cell growth: viability (%) = [(mean of absorbance value of treatment group) / (mean absorbance value of control)] ×100.

Confocal Luminescence Imaging: The **1**-PNPs-FA was dispersed in RPMI 1640 to yield 0.2 mg mL^{-1} solutions. The HeLa cells were incubated with the solution of **1**-PNPs-FA for 30 min at 37 °C. For the control group, HeLa cells were pretreated with 3 mM free FA at 37 °C for 2 h, and then incubated with **1**-PNPs-FA (0.2 mg mL^{-1}) for 30 min at 37 °C. The experiments were carried out on an Olympus FV1000 laser scanning confocal microscopy and a 60x oil-immersion objective lens. A semiconductor laser was served as excitation of the HeLa cells incubated with **1**-PNPs-FA at 405 nm. Emission was collected at 530-570 nm for the HeLa cells incubated with **1**-PNPs-FA.

Reference:

[1] C. H. Shin, J. O. Huh, M. H. Lee, Y. Do, *Dalton Trans.* **2009**, 6476.

[2] J. Brooks, Y. Babayan, S. Lamansky, P. I. Djurovich, I. Tsyba, R. Bau, M. E. Thompson, *Inorg. Chem.* **2002**, *41*, 3055.

[3] B. N. Cockburn, D. V. Howe, T. Keating, B. F. G. Johnson, J. Lewis, *J. Chem. Soc., Dalton Trans.* **1973**, 404.

[4] G. M. Sheldrick, *SHELXTL-97, A Program for Crystal Structure Refinement*; Universität of Göttingen: Germany, **1997**.

[5] B. Delley, *J. Chem. Phys.* **2000**, *113*, 7756.

[6] B. Delley, *J. Chem. Phys.* **1990**, *92*, 508.

[7] J. P. Perdew, K. Burke, M. Ernzerhof, *Phys. Rev. Lett.* **1996**, *77*, 3865.

[8] B. Delley, *Phys. Rev. B.* **2002**, *66*, 155125:1.

Table S1. Absorption data of complexes **1**-**9** in CH_2Cl_2 solution.

complex	λ_{abs}(logε) [nm]
1	265(4.85), 308(4.21,sh), 360(4.28), 396(4.06), 451(3.81,sh)
2	259(4.80), 307(4.48,sh), 360(4.28), 393(3.96), 448(3.85,sh)
3	265(4.69), 304(4.23,sh), 357(4.02), 393(3.96), 437(3.61,sh)
4	261(4.78), 301(4.24,sh), 321(4.22), 354(4.21), 386(3.98), 433(3.81,sh)
5	258(4.68), 321(4.19,sh), 354(4.14), 383(3.90), 428(3.70,sh)
6	262(4.70), 325(4.09,sh), 351(4.00), 386(3.91), 428(3.71,sh)

7	268(4.83), 320(4.39), 360(4.35), 388(4.11), 450(4.04)
8	273(4.87), 321(4.38), 368(4.37), 399(4.11), 448(4.01,sh)
9	263(4.30), 306(3.79,sh), 360(3.73), 396(3.53), 448(3.30,sh)

Table S2. HOMOs and LUMOs distributions of complexes **1-9** (gas state) at ground and excited state.

Complex	Ground-state		Excited-state	
	HOMO	LUMO	HOMO	LUMO
1	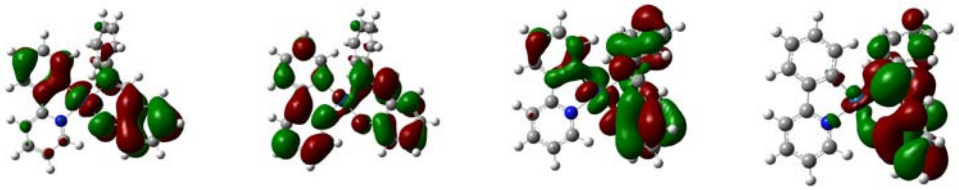			
2	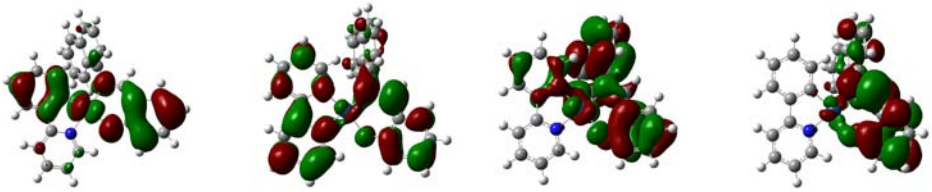			
3				
4	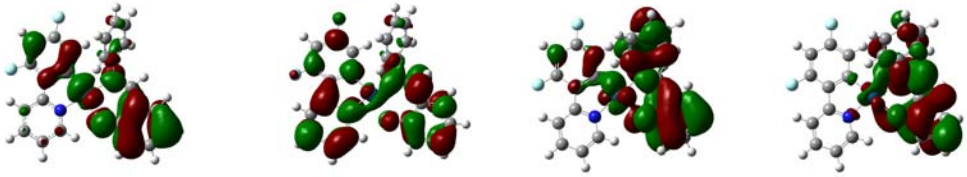			
5	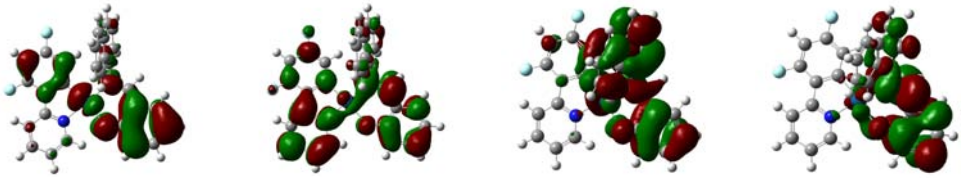			
6	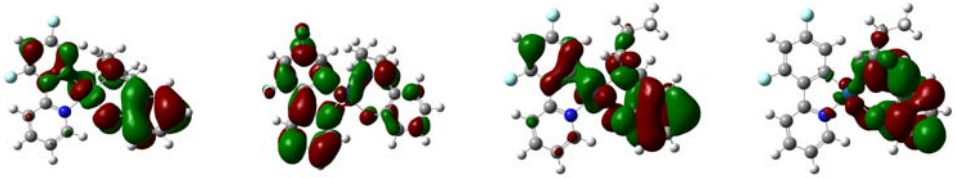			

7		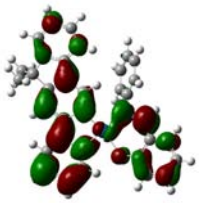	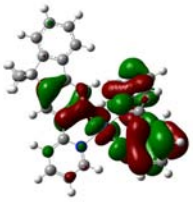	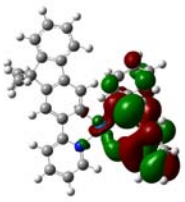
8	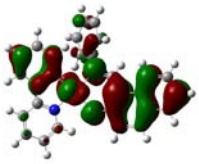	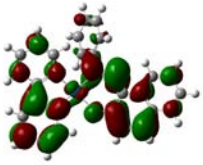	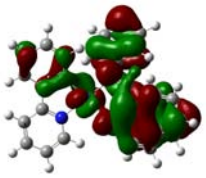	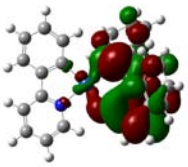
9		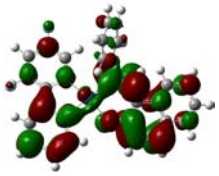	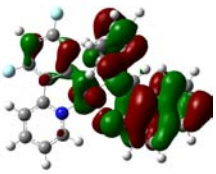	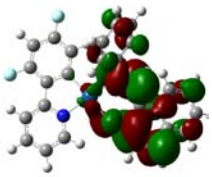

Table S3. Calculated transition nature of **1-9** in CH_2Cl_2 solution with the TDDFT method.

Complex	State	Configuration	Character
1	T_1	HOMO→LUMO (0.81)	ILCT/MLCT/LLCT
2	T_1	HOMO→LUMO (0.75)	ILCT/MLCT/LLCT
3	T_1	HOMO→LUMO (0.74)	ILCT/LLCT/MLCT
4	T_1	HOMO→LUMO (0.96)	ILCT/MLCT/LLCT
5	T_1	HOMO→LUMO (0.76)	ILCT/MLCT/LLCT
6	T_1	HOMO→LUMO (0.76)	ILCT/MLCT/LLCT
7	T_1	HOMO→LUMO (0.80)	ILCT/MLCT/LLCT
8	T_1	HOMO→LUMO (0.81)	ILCT/MLCT/LLCT
9	T_1	HOMO→LUMO (0.78)	ILCT/MLCT/LLCT

Table S4. Calculated and crystal molecular dihedral angles (°) and bond lengths (Å) of complexes **1-9**.

Complex	Dihedral angles (°) and bond lengths (Å)	At ground state	At triplet state	Crystal
1	N2-Pt-O1 to C3-C2-O1 (°) [a]	17.80	40.93	17.85
	N2-Pt-O1 to C3-C4-N2 (°) [a]	13.58	48.37	12.78
	N2-Pt-O1 to C5-C6-C7 (°) [a]	-64.35[b]	-52.52[b]	-66.25[b]
	C1-Pt (Å) [a]	2.017	2.006	2.002 (5)
	N1-Pt (Å) [a]	2.047	2.063	2.019 (4)

	N2-Pt (Å) [a]	2.066	2.017	2.026 (4)
	O1-Pt (Å) [a]	2.131	2.135	2.074 (3)
2	N2-Pt-O1 to C3-C2-O1 (°) [a]	12.16	37.77	13.12
	N2-Pt-O1 to C3-C4-N2 (°) [a]	9.43	36.06	9.88
	N2-Pt-O1 to C5-C6-C7 (°) [a]	-76.00[b]	-70.73[b]	-75.77[b]
	C1-Pt (Å) [a]	2.024	2.010	2.009 (6)
	N1-Pt (Å) [a]	2.049	2.060	2.023 (5)
	N2-Pt (Å) [a]	2.075	2.049	2.029 (5)
	O1-Pt (Å) [a]	2.132	2.130	2.084 (4)
3	N2-Pt-O1 to C3-C2-O1 (°) [a]	26.34	38.03	28.08
	N2-Pt-O1 to C3-C4-N2 (°) [a]	20.35	32.14	20.02
	N2-Pt-O1 to C5-C6-C7 (°) [a]	--[c]	--[c]	--[c]
	C1-Pt (Å) [a]	2.010	2.004	2.003 (7)
	N1-Pt (Å) [a]	2.047	2.072	2.014 (7)
	N2-Pt (Å) [a]	2.055	2.002	2.015 (8)
	O1-Pt (Å) [a]	2.133	2.137	2.063 (5)
4	N2-Pt-O1 to C3-C2-O1 (°) [a]	-10.07[b]	-41.45[b]	--[c]
	N2-Pt-O1 to C3-C4-N2 (°) [a]	-14.81[b]	-49.24[b]	--[c]
	N2-Pt-O1 to C5-C6-C7 (°) [a]	113.79	126.09	--[c]
	C1-Pt (Å) [a]	2.013	2.003	--[c]
	N1-Pt (Å) [a]	2.068	2.060	--[c]
	N2-Pt (Å) [a]	2.045	2.019	--[c]
	O1-Pt (Å) [a]	2.122	2.128	--[c]
5	N2-Pt-O1 to C3-C2-O1 (°) [a]	-12.20[b]	-38.66[b]	-10.21[a]
	N2-Pt-O1 to C3-C4-N2 (°) [a]	-9.39[b]	-38.88[b]	-7.80[a]
	N2-Pt-O1 to C5-C6-C7 (°) [a]	104.84	118.43	106.69
	C1-Pt (Å) [a]	2.019	2.008	1.991 (8)
	N1-Pt (Å) [a]	2.048	2.056	2.025 (6)
	N2-Pt (Å) [a]	2.078	2.050	2.034 (6)
	O1-Pt (Å) [a]	2.119	2.127	2.058 (5)
6	N2-Pt-O1 to C3-C2-O1 (°) [a]	27.52	-36.80[b]	--[c]
	N2-Pt-O1 to C3-C4-N2 (°) [a]	21.45	-33.32[b]	--[c]
	N2-Pt-O1 to C5-C6-C7 (°) [a]	--[c]	--[c]	--[c]
	C1-Pt (Å) [a]	2.005	2.004	--[c]

	N1-Pt (Å) [a]	2.045	2.069	--[c]
	N2-Pt (Å) [a]	2.055	2.001	--[c]
	O1-Pt (Å) [a]	2.125	2.131	--[c]
7	N2-Pt-O1 to C3-C2-O1 (°) [a]	17.54	41.00	--[c]
	N2-Pt-O1 to C3-C4-N2 (°) [a]	13.61	48.28	--[c]
	N2-Pt-O1 to C5-C6-C7 (°) [a]	-64.88[b]	-52.24[b]	--[c]
	C1-Pt (Å) [a]	2.020	2.007	--[c]
	N1-Pt (Å) [a]	2.045	2.061	--[c]
	N2-Pt (Å) [a]	2.068	2.018	--[c]
	O1-Pt (Å) [a]	2.130	2.135	--[c]
8	N2-Pt-O1 to C3-C2-O1 (°) [a]	22.78	42.65	22.86
	N2-Pt-O1 to C3-C4-N2 (°) [a]	19.59	48.33	21.37
	N2-Pt-O1 to C5-C6-C7 (°) [a]	-55.34[b]	-52.33[b]	-66.32[a]
	C1-Pt (Å) [a]	2.013	2.008	1.980 (5)
	N1-Pt (Å) [a]	2.046	2.059	2.009 (4)
	N2-Pt (Å) [a]	2.059	2.017	2.004 (4)
	O1-Pt (Å) [a]	2.133	2.130	2.065 (4)
9	N2-Pt-O1 to C3-C2-O1 (°) [a]	-22.88[b]	-42.00[b]	--[c]
	N2-Pt-O1 to C3-C4-N2 (°) [a]	-19.80[b]	-40.58[b]	--[c]
	N2-Pt-O1 to C5-C6-C7 (°) [a]	112.62	63.08	--[c]
	C1-Pt (Å) [a]	2.010	2.006	--[c]
	N1-Pt (Å) [a]	2.045	2.053	--[c]
	N2-Pt (Å) [a]	2.060	2.031	--[c]
	O1-Pt (Å) [a]	2.125	2.118	--[c]

[a] See Scheme S1. [b] Minus denotes the opposite distortion direction. [c] No crystal data.

Table S5. The optimized ground-state and triplet-state geometries of complexes **1-9**.

Complex	Ground-state geometry	Triplet-state geometry
1	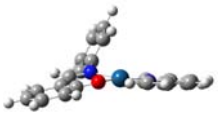	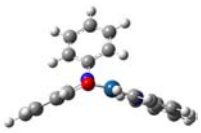
2		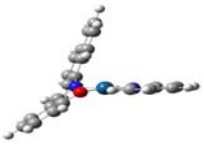

3	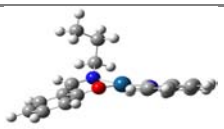	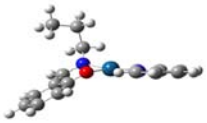
4		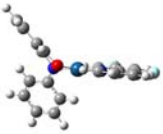
5	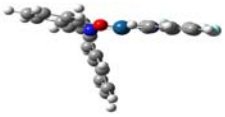	
6	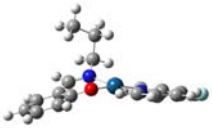	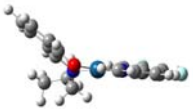
7	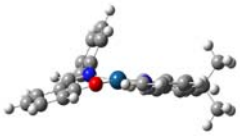	
8	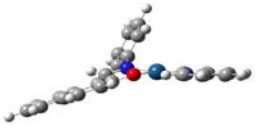	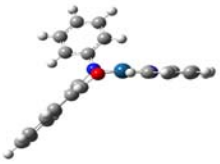
9	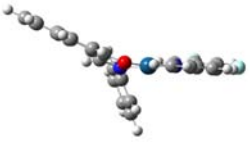	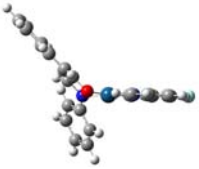

Table S6. The calculated HOMO and LUMO orbitals at the triplet state (based on corresponding crystal structures).

Complex	HOMO	LUMO
1		
2	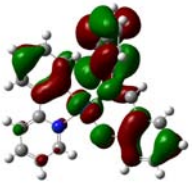	

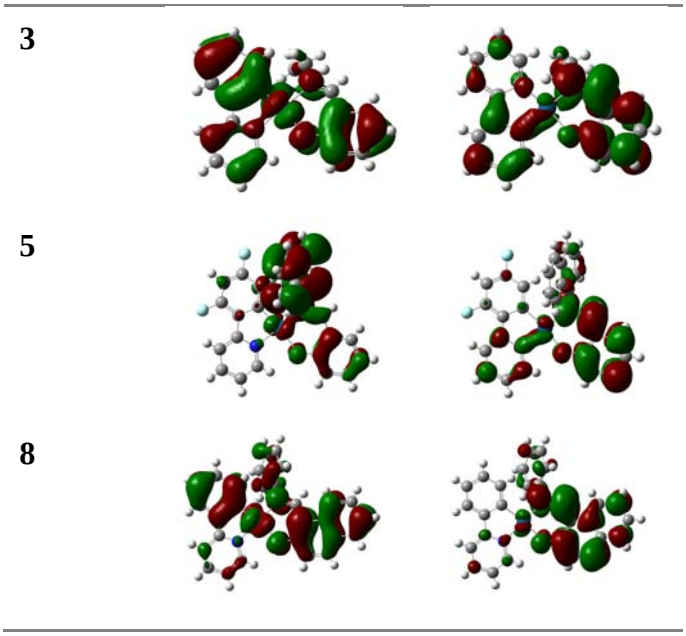

Table S7. The singlet-state energy levels of the cyclometalated and ancillary ligands

Ligand	ppy	dfppy	Fiq	L1	L2	L3	L4
S_1, cm^{-1}	32680	34014	27933	25974	24390	28736	20619

Scheme S1. The structure of platinum complex.

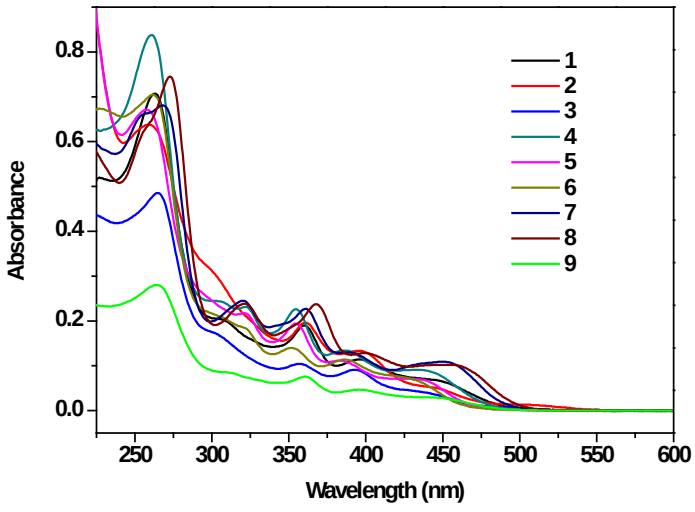

Figure S1. Absorption spectra of **1-9** (1×10^{-5} mol L^{-1}) at room temperature in CH_2Cl_2 solution.

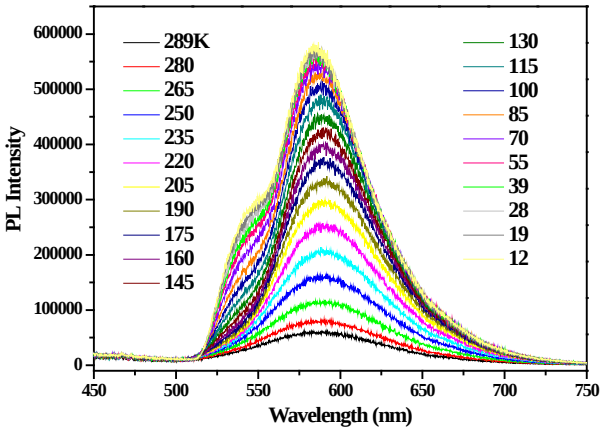

Figure S2. Emission spectra of **3** (crystal) at different temperatures.

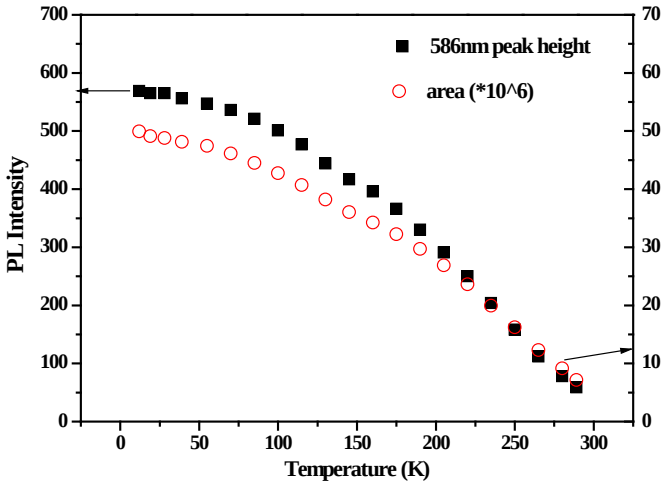

Figure S3. Emission peak height and area of **3** (crystal) at different temperatures.

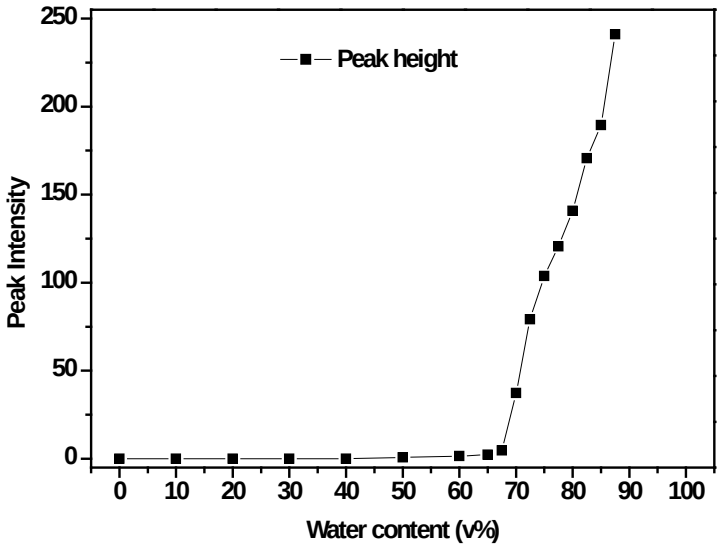

Figure S4. Emission peak height of **1** in THF/water mixtures.

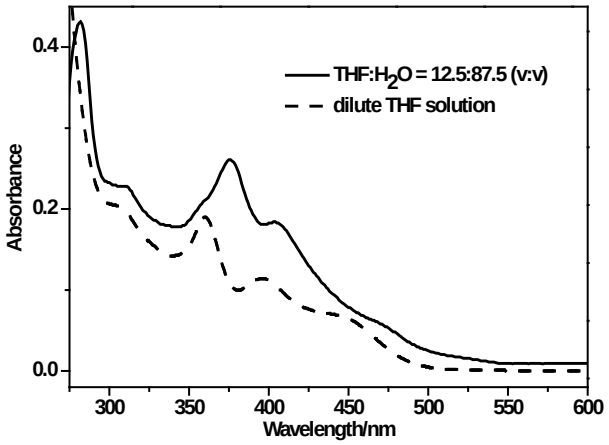

Figure S5. Absorption spectra of **1** (1×10^{-5} mol L^{-1}) in THF and THF/water mixture (87.5% volume fractions of water).

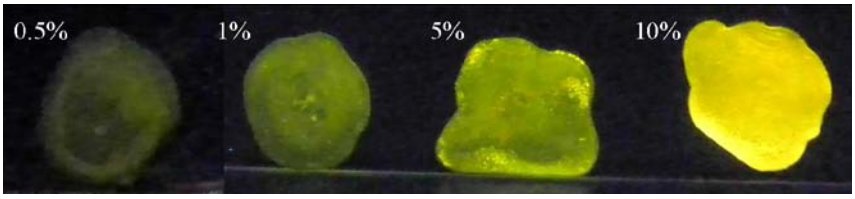

Figure S6. Luminescence photographs of the solid poly(methyl methacrylate) (PMMA) film doped with different contents of **1**.

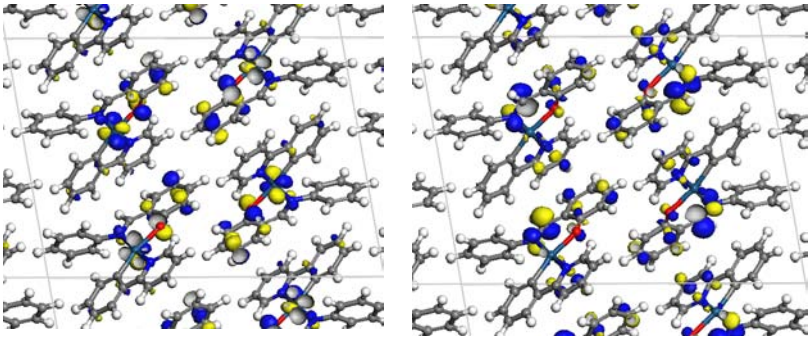

Figure S7. Calculated HOMO (left) and LUMO (right) distributions of **1** in crystal state.

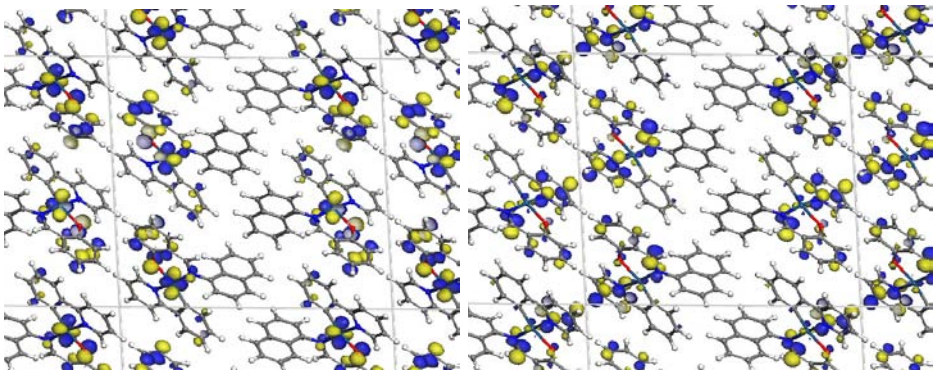

Figure S8. Calculated HOMO (left) and LUMO (right) distributions of **2** in aggregation state.

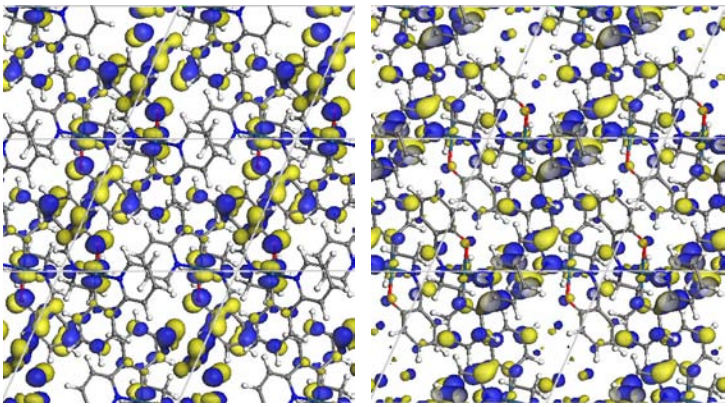

Figure S9. Calculated HOMO (left) and LUMO (right) distributions of **3** in aggregation state.

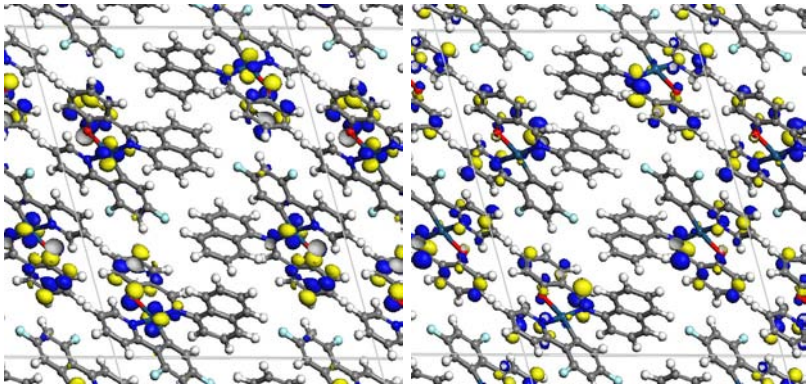

Figure S10. Calculated HOMO (left) and LUMO (right) distributions of **5** in aggregation state.

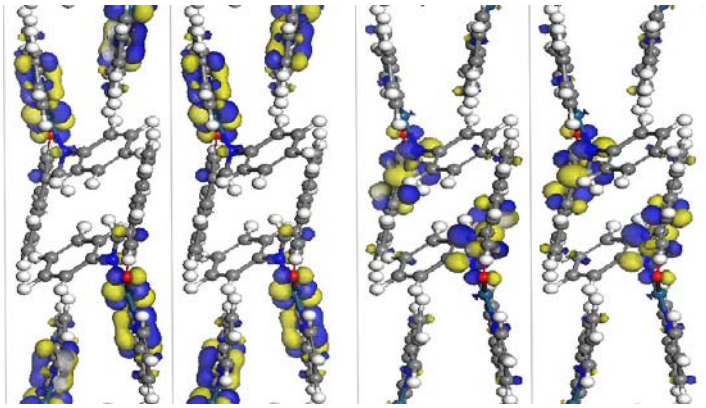

Figure S11. Calculated HOMO (left) and LUMO (right) distributions of **8** in aggregation state.

To explain the significant difference in emission properties, the singlet energy levels of the cyclometalated and ancillary ligands were estimated by referring to wavelengths of the UV-vis absorbance edges of the diketonate ligands (see Figure S12). The corresponding data were provided in Table S7.The wavelengths of UV-vis absorbance edges of ppy, dfppy, Fiq, L1, L2, L3 and L4 are 306, 294, 358, 410, 348 and 485 nm, respectively, indicating that their corresponding singlet energy levels are 32680, 34014, 27933, 25974, 24390, 28736 and 20619 cm^{-1}, respectively. The singlet energy level of ancillary ligand lies lower than the corresponding cyclometalated ligand. Thus, its luminescence is dominated by ancillary ligand, leading to inefficient emission in solution.

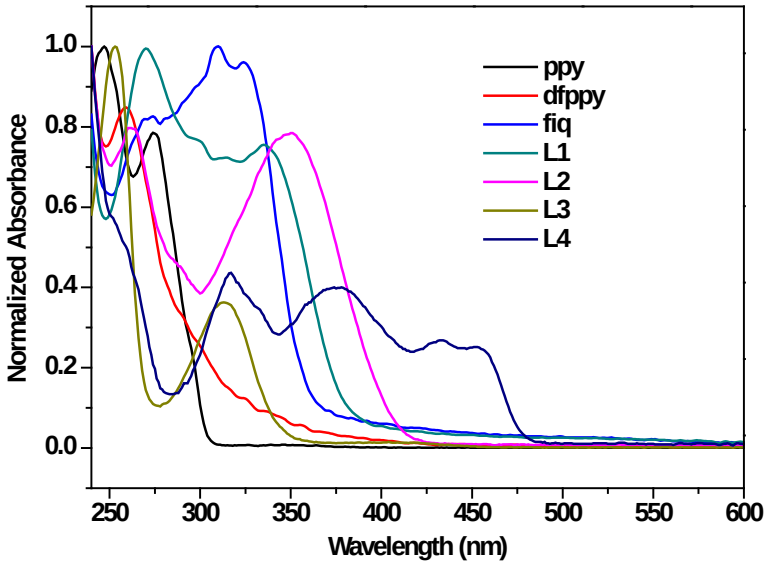

Figure S12. Absorption spectra of cyclometalated and ancillary ligands at room temperature in acetonitrile solution.

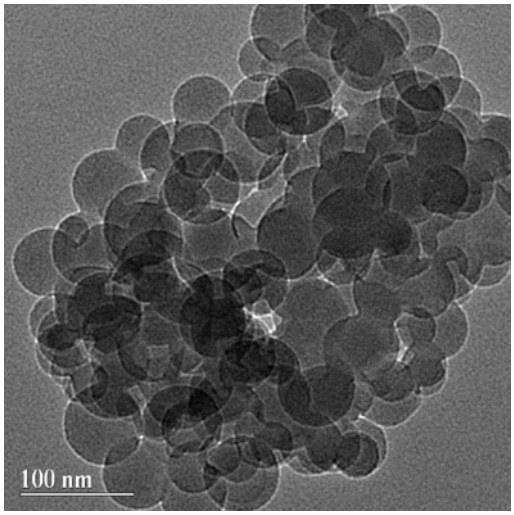

Figure S13. TEM image of **1**-PNPs-FA dispersed in water.

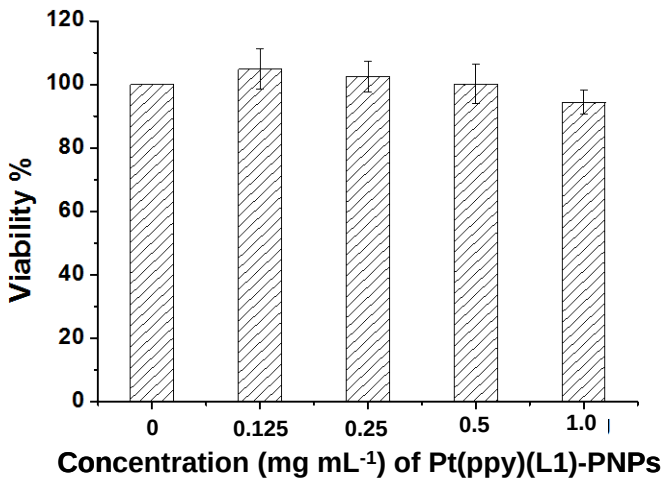

Figure S14. Cell viability values (%) assessed by MTT proliferation test versus incubation concentrations of **1**-PNPs-FA. HeLa cells were cultured in the presence of 0-1.0 mg mL^{-1} **1**-PNPs-FA at 37 °C for 24 h.

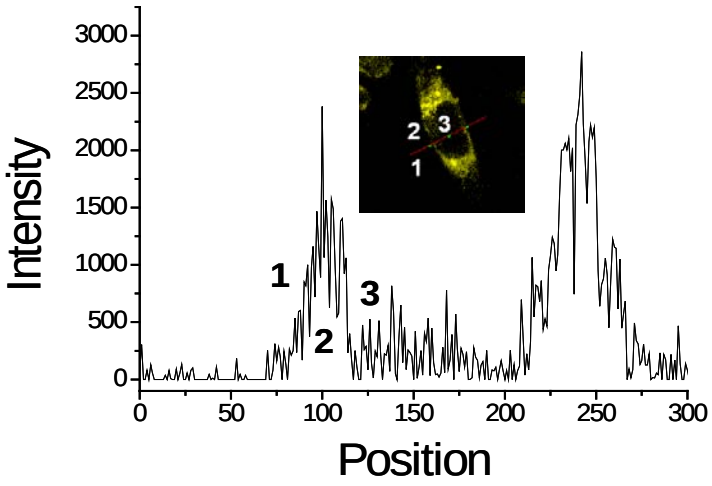

Figure S15. Confocal luminescence images (insert) and luminescence intensity profile (across the line shown in the insert image) of the living HeLa cells.

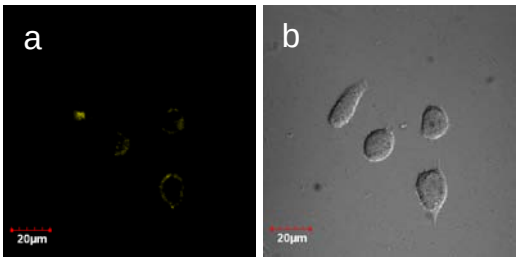

Figure S16. Confocal luminescence (a) and bright-field (b) images of MCF-7 cells incubated with 0.2 mg mL^{-1} **1**-PNPs-FA for 30 min. The excitation wavelength is 405 nm.